

## Short Term Variations of Galactic Cosmic Rays Observed with GRAPES-3 Muon Telescopes

T.Nonaka<sup>a</sup> S.K.Gupta<sup>b</sup> Y.Hayashi<sup>a</sup> N.Ito<sup>a</sup> A.Jain<sup>b</sup> A.V.John<sup>b</sup> S.Karthikeyan<sup>b</sup> S.Kawakami<sup>a</sup>  
H.Kojima<sup>c</sup> K.Matsumoto<sup>a</sup> Y.Matsumoto<sup>a</sup> T.Matsuyama<sup>a</sup> D.K.Mohanty<sup>b</sup> P.K.Mohanty<sup>b</sup>  
S.D.Morris<sup>b</sup> T.Okuda<sup>a</sup> A.Oshima<sup>a</sup> B.S.Rao<sup>b</sup> K.C.Ravindran<sup>b</sup> M.Sasano<sup>a</sup> K.Sivaprasad<sup>b</sup>  
B.V.Sreekantan<sup>b</sup> H.Tanaka<sup>a</sup> S.C.Tonwar<sup>b</sup> K.Viswanathan<sup>b</sup> T.Yoshiyoshi<sup>a</sup>

(a) Graduate School of Science, Osaka City University, Osaka 558-8585, Japan

(b) Tata Institute of Fundamental Research, Homi Bhabha Road, Mumbai 400005, India

(c) Nagoya Women's University, Nagoya 467-8610 Japan

Presenter: Toshiyuki Nonaka (nonaka@alpha.sci.osaka-cu.ac.jp), jap-nonaka-T-abs1-sh26-oral

A large area multi-directional muon telescope is operated as a part of the GRAPES-3 Air Shower experiment at Ooty (N11.4°, E76.7° and 2200m altitude). The muon detector has an area of 560 m<sup>2</sup> and threshold energy of 1.0 GeV. Due to large detector size, a very large number of muons,  $\sim 1.7 \times 10^8$ , per hour are detected. The design of the muon detector allows simultaneous measurement of muon intensity from 225 directions. Therefore it enables us to make a 2-dimensional map of intensity variation of cosmic ray with energy of  $\sim 70$  GeV. In general, due to a higher median rigidity of the response, the muon telescope can detect small scale anisotropy more precisely as compared to a neutron monitor. It is also useful for space weather forecasting. Here we analyze the cosmic ray storm events observed during the period, 2001-2002. A number of Loss-Cone Precursor decreases were detected during this period. The association rate for Forbush decrease (Fd) and correlation with magnitude of Fd are also discussed.

### 1. Introduction

It is well-known that several kinds of anisotropy of GCR emerge during the period when a shock wave in interplanetary space is approaching the observer. Using neutron monitors and muon detectors, Nagashima and Fujimoto[1] had pointed out that small angular scale anisotropy near the direction of Interplanetary Magnetic Field (IMF) are due to “Loss-Cone” effect between turbulent region behind the shock and the observer. This phenomenon is called Loss-Cone Precursor Decrease(LCPD). It was also pointed by them and by many others that this LCPD can be used for space weather forecasting [2,3].

Since the LCPD anisotropy has small angular scale structure  $\sim 30^\circ$ , observations requires relatively good angular resolution and high statistical accuracy. Recent success in 2-Dimensional observation of LCPDs are mainly from observation by muon telescope/hodoscope with angular resolution smaller than  $\sim 10^\circ$  [4,5,6]. Accumulation of LCPD events, is making it possible to extract average features of LCPDs and correlations with the following Forbush decrease (Fd) with muon telescope observations.

### 2. GRAPES-3 Muon Telescopes

A large extensive air shower (EAS) array, GRAPES-3 has been installed at Ooty (2200m altitude, 11.4°N, 76.7°E) for detailed studies on energy spectrum and composition of primary cosmic rays over the energy range  $3 \times 10^{13}$ - $3 \times 10^{16}$  eV. The array consists of electron density detectors and 16 multi directional muon telescopes. The muon telescope consists of proportional counters which have dimensions 10cm×10cm×600cm. Each detector module has four layers of 58 proportional counters. Successive layers are placed in orthogonal direc-

tions. to enable measurement of the arrival direction of penetrating muon track. Threshold energy for vertical muons is 1 GeV. The arrival direction of detected muon is categorized into  $15 \times 15$  directional cells as shown in Fig.1. The total area of 16 muon telescopes is  $560\text{m}^2$ . Statistical accuracy of hourly count in each cell is  $0.1\% \sim 0.3\%$ .

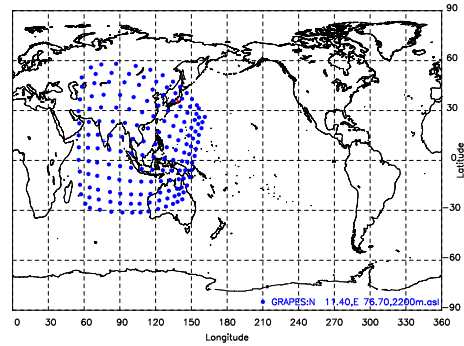
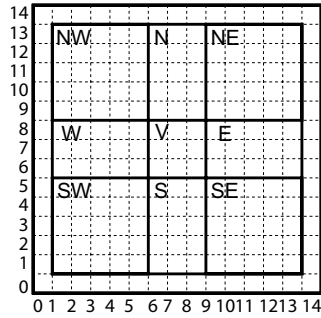


**Figure 1.**  $15 \times 15$  cells in FOV. The FOV was reconfigured into 9 (NW,N,NE,W,V,E,SW,S,SE)

**Figure 2.** Asymptotic Viewing direction at the median rigidity of muon telescope in geographical coordinate

### 3. Observation and Analysis

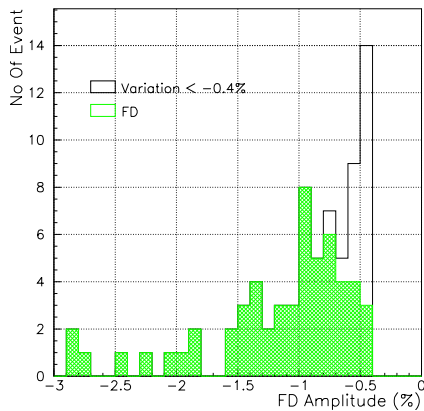


**Figure 3.** Distribution of the amplitude of observed Forbush decreases

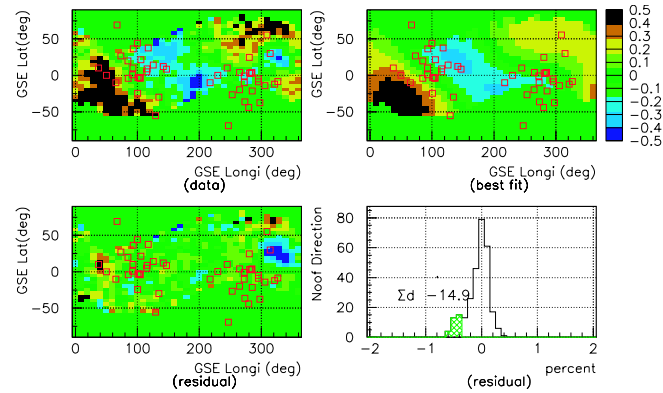


**Figure 4.** An example of subtraction of background anisotropy. (2001/3/25-26)

From 1 March 2001 to 31 December 2002, a total 659 days of data were analyzed. Fd events were selected from this dataset. For the analysis, FOV was divided into 9 directional cells as shown in Fig1. From hourly count rate data for these 9 cells, the Fd events were searched for. Fd candidate were selected under the condition that any one of the 9 cells showed a deficit greater than 0.4% between minimum intensity of current 24 hours and the up-coming 24 hour period. The start-time of Fds were defined by the time when intensity decreased lower than lowest intensity in current 24 hours. The amplitude of Fd is defined by maximum deficit among the data of 9 cells. The empty histogram in black, in Fig 3 corresponds to an Fd candidate as described above. Some of those events with amplitude smaller than 0.6% were rejected during this analysis due to a gradual slope. The

remaining 56 events were selected as Fds in this analysis. The distribution of amplitudes is displayed in Fig 3. The Loss-Cone Precursor Decrease(LCPD) were searched from these 56 events.

It is already known from earlier works [4] that some of the LCPD anisotropy seems to have a relatively broad 2-dimension structure. In such a case, the limited FOV of the telescope, does not permit an accurate measurement of amplitude of the anisotropy. To evaluate amplitude correctly, it is necessary to estimate the solar diurnal anisotropy. for this purpose the data are separated into units of 24 hour duration (start from 5h in UTC) and each unit was categorized into one of the three types “A”, ”B” and “N” using the following criteria.

(A): Data unit include start of Fd and following two data units were defined as category “A”

(B): Data units includes period before the start of the Fd. Two data units prior to the unit which includes start of Fd were defined as category “B”. If a unit is included in “A” also, the unit is categorized into “B’”.

(N): Data units those were not included “A” or “B”

Number of data sets in each category were 136 units in “A”, 84 units in “B”, 27 units in “B’” and 412 units in “N” data.

### 3.1 Evaluation of anisotropy near IMF direction

We have used the central 169 out of 225 directional cells as the FOV. Loss-Cone(LC) search were done for all category of data. In this analysis, relative intensity in the data unit is used hereafter. The observing direction of each cell is defined as asymptotic arrival direction of median rigidity particles. Shape of large scale anisotropy such as solar diurnal anisotropy or Swinson flow can be estimated using data points in the direction of GSE longitude  $0^\circ \sim 270^\circ$ . The estimations were done by fitting a spherical harmonic function to the observed data. Up to second order harmonics and linear function of time were used for fitting. The second harmonics is to reduce the residuals due to approximate knowledge of the observing direction. Common variation was assumed as a linear function of time. In the case of data in category “A”, a total of 17 sets could not be fitted due to complicated intensity variation caused by FD. After obtaining the shape of diurnal anisotropy, residual between best fit function and the data are calculated for each data point. At each  $5^\circ$ , mean residuals are calculated using data points within the opening angle of  $5^\circ$ .

The top two panel of Fig 4 are an example of observed anisotropy and best fit large scale anisotropy estimated by the method described above. Bottom two panels on Fig 4 show a residual after subtracting best fit anisotropy from observed data. Bottom right panel shows the histogram of residual values in the direction of GSE  $270^\circ \sim 360^\circ$ . From eye-scan analysis, it is known that for LCPD events, the histograms have significant distribution below  $-0.35\%$ . Thus in this analysis we defined the integrated value of this histogram below  $-0.35\%$  as  $\sum d_{0.35}$ . Using this  $\sum d_{0.35}$  parameter, it becomes possible to evaluate local anisotropy near IMF more objectively even with data from a single station. Following table lists frequency of observed  $\sum d_{0.35}$  value in each category,

$\sum d_{0.35}$ value	Observed in “N” Data	Observed in “B” Data
$\sum d_{0.35} \leq -10$	13 days/410 N data	13/84 B data
$\sum d_{0.35} \leq -20$	8 days/410 N data	8/84 B data
$\sum d_{0.35} \leq -30$	5 days/410 N data	3/84 B data
$\sum d_{0.35} \leq -40$	3 days/410 N data	3/84 B data
$\sum d_{0.35} \leq -50$	2 days/410 N data	3/84 B data

**Table 1.** Frequency of observing  $\sum d_{0.35}$  under several condition.

## 4. Result and Discussion

During 13 days which show  $\sum d_{0.35} < -10.0$  were found from 84 days categorized “B”. With same conditions 13 days were found from category “N”. Thus it is clear that days showing large  $\sum d_{0.35}$  value are concentrated before an Fd rather than “N”(Normal) days. The chance probability to get this result is less than  $10^{-5}$ . By combining 4 events observed in B' data, the correlation between Fd amplitudes were obtained as Fig 5. In

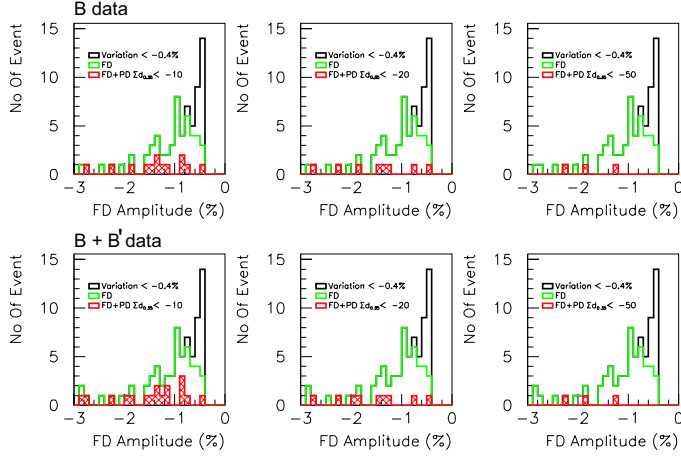


**Figure 5.** Frequency of Fds which follows LCPD evaluated by  $\sum d_{0.35}$  parameter as displayed in the same histogram.

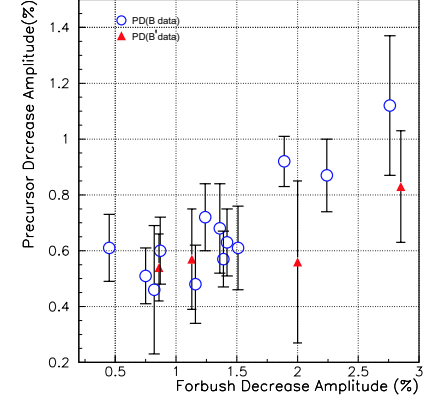


**Figure 6.** relation between FD amplitude and amplitude of LCPD ( $\sum d_{0.35} \leq -10$ )

Fig 5, one can see a clear trend to observe LCPD with greater frequency before a large Fd. These results which were expected from LCPD model proposed by Nagashima et.al[2,3]. Fig 6 shows correlation between maximum of LC depth and following Fd amplitude. This trend is also expected for the model in [2,3].

## 5. Acknowledgements

We thank D.B. Arjunan, A.A. Basha, G.P. Francis,I.M. Haroon, V. Jeyakumar,K. Manjunath, B. Rajesh, K. Ramadass, C. Ravindran, and V. Viswanathan for help in construction and operation of GRAPES-3 experiment. We acknowledge partial financial support from Ministry of Education and Science, Government of Japan. We thank N.K. Mondal and colleagues for loan of proportional counters of KGF experiment.

## References

- [1] K.Nagashima and K.Fujimoto et al.,Planet space sci (1992) 40 1109
- [2] K.Munakata et.al.,J,Geophys.Res A (2000) 105 27457
- [3] A. Belov and J.W Bieber et al.,Proc.27th ICRC (2001)
- [4] T.Nonaka et.al.,Proc.28th ICRC (2003),v6,3569
- [5] K.Fujimoto et.al., Proc.28th ICRC (2003),v6,3565
- [6] K.Munakata et.al.,Geophys.Res.Lett (2005) 32 L03S04